DEVELOPMENT OF PIEZO SMART MATERIALS AND DEVICES AT NAL

B.Sahoo, V.A. Jaleel and P.K.Panda*
Materials Science Division,
National Aerospace Laboratories, P.B.No.1779, Kodihalli, Bangalore-17

ABSTRACT

Materials used for both sensing and actuation are known as smart materials. Ceramic materials such as Lead Zirconate Titanate (PZT) and Lead Magnesium Niobate (PMN) are widely used for various smart applications such as sensing and control of aero structures. PZTs are solid solutions of Lead Zirconate and Lead Titanate. The piezo properties are maximum near Morphotropic Phase Boundary (MPB) and are further enhanced by addition of suitable donor dopants such as La^{3+}, Nb^{5+}, Nd^{3+} etc. At NAL, PZT powders of high piezo-coefficient (d_{33}=595-600 pC/N) are prepared by wet-chemical route. The powders were characterized for their ferroelectric, piezoelectric and dielectric properties. Similarly, PMN is a very high dielectric relaxor material (K=20,000 at RT) widely used for making capacitors and electrostrictive actuators. Pyrochlore free PMN powder was prepared by modified "columbite" route. The effect of different lead precursors in the formation of PMN powder was also studied. The dielectric constant was measured at room temperature and found to be 10,335 at 100Hz while it was 20,000 at 4.5MHz. Few Multi-layered (25-50 layers) stacks were also fabricated using the synthesized powder. The displacement and free strain of the stacks were measured using a strain sensor. The maximum displacement and the free strain were found to be 20μm and 0.1% respectively at 450V. Currently, efforts are being made to prepare the above materials in 1Kg/batch and fabrication of actuators/sensors by tape-casting technique to minimize the thickness of each layer ~50μm suitable for low operating voltage.

INTRODUCTION

Lead Zirconate Titanate (PZT) is an important material used for "smart" applications i.e. for both sensing as well as for actuating purpose in the form of sensors and actuators. It has excellent piezoelectric properties such as high piezo-electric charge constant (d_{33}), high coupling coefficient, high dielectric constant etc. and is widely used as actuators and sensors, as sonar transducers, as accelerometers, in inkjet printers, gas igniter etc. It is a solid solution of two perovskites, lead zirconate ($PbZrO_3$) and lead titanate ($PbTiO_3$). PZT with zirconia rich compositions are rhombohedral in nature where as titania rich compositions are tetragonal in nature. The compositions where both the two phases coexist are known as morphotropic phase boundary (MPB)(ref.1-4). The high piezo properties exist at this phase boundary region (ref.5-8).

The properties of PZTs are further modified by the introduction of different dopants in "A" or "B" sites of the perovskite structure ABO3 (ref.9). These dopants are mainly of two types i.e. "donor" dopants such as La^{3+}, Nd^{3+},B^{3+},Nb^{5+}, Ta^{5+}, W^{6+}, Th^{4+} and Sb^{5+} which produce "soft" PZTs or "acceptor" dopants such as K^{+}, Na^{+},Sc^{3+}, Mg^{2+}, and Fe^{3+} which produce "hard" PZTs. The soft dopants facilitate the domain wall motion and enhance easy reorientation of the dipoles during poling, thereby; the electronic properties of these PZTs are very high compared to undoped PZTs. The soft PZTs are widely used for various applications such as actuators and sensors (ref.10-14), sonar transducers (ref.15), ultrasonic motor (ref.16), accelerometers, in drug delivery systems, in smart toilets, in gas igniters, in inkjet printers (ref.17) etc. The use of PZT materials is unlimited because these materials can be tailor made with a wide range of properties by varying the compositions with different dopants to suit the desired applications. These materials are prepared by various methods such as "mixed oxide" (ref.18-20) as well as by different chemical routes (ref.21-26). Wet chemical method is a well known process for the

preparation of PZT powders due to the merits of easy compositional control, better homogeneity and low processing temperature compared to the conventional solid-state "mixed oxide" process. Lead magnesium niobate (PMN), $Pb(Mg_{1/3}Nb_{2/3})O_3$, is a relaxor ferroelectric material with high dielectric constant (K~20,000) and large electric-field-induced strain (ref.27-32). Therefore, PMN is extensively used as capacitor and also as electrostrictive actuators. However, the main drawback in producing PMN material is the formation of a low dielectric constant (K~200) lead niobate "pyrochlore" phase, which degrades the properties of the PMN powders. Pyrochlore phase is invariably formed during the direct synthesis of PMN powder by mixed oxide route. To overcome this problem Swartz and Shrout (ref.33) has attempted a two-step process commonly known as "columbite" route where MgO and Nb_2O_5 are pre reacted to form columbite ($MgNb_2O_6$) which is then reacted with PbO to form PMN powder. Swartz et all (ref.27) also prepared pyrochlore free PMN powder by using excess MgO. Other investgators (ref.34-36) have confirmed the superiority of the two-stage synthesis over direct method and also highlighted the importance of excess PbO (ref.37,38) on the yield of perovskite phase. PMN is also synthesized by various chemical processing routes such as sol-gel (ref.39-41), combustion synthesis (ref.42,43), EDTA gel (ref.44), citrate gel (ref.45), coprecipitation (ref.46), molten salt synthesis (ref.47), partial oxalate method (ref.48) and also by polymeric precursor (ref.49,50) methods. The above chemical routes have potential to form pyrochlore free PMN powders due to better homogeneity, compositional control and lower processing temperature etc., therefore, are preferred over solid state reaction process.

In this paper, a preliminary study on preparation of PZT powders with compositions near MPB region as well as with donor dopants and fabrication and characterisation of multi-layered stacks are presented. The powders were prepared by wet-chemical method to achieve compositional homogeneity, stoichiometry and fine particle size distribution necessary to obtain better properties. The MPB composition was identified by X-Ray Diffraction (XRD) technique and the effect of dopants on polarization behavior was studied from the hysteresis loop obtained for different compositions. Few multilayered stacks were fabricated and the percentage free strain was also measured. Similarly a comparative study on preparation of pyrochlore free PMN powders is presented using different lead precursors such as lead hydroxide, lead acetate and lead formate. The powders are prepared by both direct and columbite methods and also with stoichiometric as well as with 3% excess MgO in order to optimize the processing condition for preparation of pyrochlore free PMN powder.

EXPERIMENTAL PROCEDURE

Preparation of PZT powders

Analytical grade lead nitrate (99.5%) zirconium oxychloride (99.9%), titanium tetrachloride (99%) and lanthanum nitrate (99.9%) were used as starting chemicals for the preparation of PZT powders. The combined salt solution with excess lead precursor along with dopant solution was gelled by raising the pH up to 8.5 with suitable gelling agent. The gel was dried and calcined in the temperature range of 750-900°C for 1-4 hours. After calcination, the powders were de-agglomerated and PZT phase formation was confirmed by X-Ray Diffraction (XRD),(M/s. Phillips, Holand). The average particle size d_{50} of the calcined powder was measured using the particle size analyzer (Sedigraph 5100, M/s. Micromeritics, USA). The powder was granulated, compacted and sintered in the temperature range of 1050-1250°C for 2h in a closed lead rich atmosphere. Sintered pellets were leveled, polished, electroded and finally poled in a dc field at 2kV/mm in a silicone oil bath for 30 minutes. The linear piezo-electric strain coefficient (d_{33}) was measured using a piezo-meter (Model PM-35, M/s. Take control, UK).

Preparation of PMN powders

Reagent grade lead nitrate, lead acetate, magnesium nitrate, basic magnesium carbonate and niobium pentaoxide were used as recursors. Lead formate was prepared by dissolving the precipitated lead hydroxide in appropriate amount of formic acid. PMN powders were prepared by modified columbite route with 3% excess MgO using three different lead precursors such as lead hydroxide, lead acetate and lead formate. In this process, a required amount of basic $MgCO_3$ (with 3% excess MgO) was converted into its oxalate. Nb_2O_5 powder was then dispersed in this solution and evaporated to dryness. This powder was calcined at1050°C/6h to form columbite and the phase purity was comfirmed by XRD analysis. The coulmbite was reacted with calculated amount of three different lead precursors namely lead hydroxide, lead acetate and lead formate at 800°C/4h. The resultant products from the three different lead precursors were analyzed by XRD for the phases present. Pyrochlore free PMN powder obtained was compacted and sintered at 1150°C/2h. Sintered pellets were leveled, polished, electroded and the dielectric constant was measured by varying the frequency from100Hz-5MHz using an impedance bridge.

RESULTS AND DISCUSSION (PZT)

The particle size distribution curve of calcined, grounded PZT powders is shown in Fig. 1. The curve indicates a narrow distribution of powder particles and d_{50} was found to be 1μm. A typical SEM picture of chemically etched PZT sintered pellet is shown in Fig. 2. It is observed from the picture that grains are regular in shape with a diameter of 1–2 μm in range.

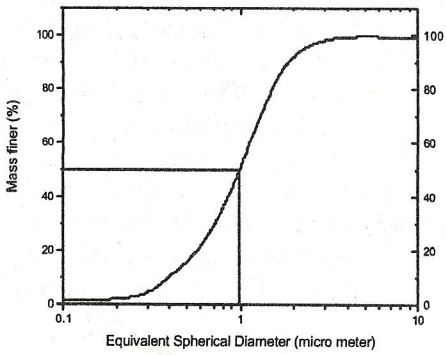

Fig.1. A typical particle size distribution of calcined PZT powder

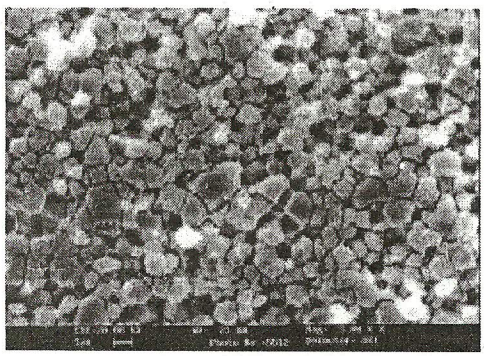

Fig.2. Typical SEM picture of PZT sintered body

Identification of Morphotropic Phase Boundary (MPB)

Morphotropic phase boundary (MPB) represents an abrupt structural change within a solid solution with variation in composition but nearly independent of temperature. Usually, it occurs because of the instability of one phase against another at a critical composition where the two phases are energetically very similar but structurally different and, thus, the mechanical strain to preserve one phase against the other is relaxed (or softened) (ref.4). Thus, in the case of solid solutions of ferroelectric compositions, many physical and electrical properties may change markedly at the MPB due to the contributions of the increased number of property coefficients at the MPB.

In case of PZT, MPB composition lies in the range of 48–54 mol% of zirconia (ref.6,7). However, the exact range varies with different precursors, processing conditions, etc. Therefore,

in order to identify the MPB composition in our system, five compositions with mole ratios of Zr/Ti = 48/52, 50/50, 52/48, 53/47 and 54/46 were studied.

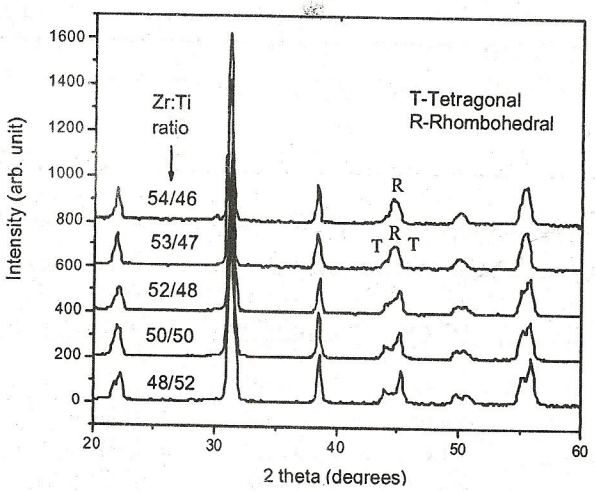

Fig.3 XRD patterns of PZT samples with Zr/Ti mole ratios

The XRD patterns of all five compositions were shown in Fig.3. The tetragonal and rhombohedral phases of the PZT compositions were identified by analyzing the peaks [0 0 2 (tetragonal), 2 0 0 (tetragonal), 2 0 0 (rhombohedral)] in the 2è range of 43–46. In XRD pattern of PZT (48/52), the absence of rhombohedral (2 0 0) peak and the split in two tetragonal peaks confirms the presence of pure tetragonal phase. As the zirconium concentration increases, the tetragonal splitting diminishes and rhombohedral peak appears, finally in composition at Zr/Ti ratio of 54/46, a pure rhombohedral phase is observed. The composition 53/47 has good amount of both tetragonal and rhombohedral phases present was identified as MPB region, which has very good properties. Therefore, the PZT (53/47) composition was selected for further study for the effects of dopants on dielectric, piezoelectric and ferroelectric polarization studies.

Piezoelectric and dielectric properties

The ferroelectric piezoelectric and dielectric properties of the four undoped compositions are shown in Table-1. From the Table-1, it is observed that the remnant polarization (Pr), piezoelectric constant (d_{33}) and dielectric constant (K) increases with increase in zirconia concentration. This could be due to the effect of co existence of tetragonal and rhombohedral phase in MPB region (ref.51).

The ferroelectric, piezoelectric and dielectric properties of PZT(53/47) doped with lanthanum, neodymium or their combinations are presented in Table-2. From this table, it is observed that the d_{33} values of doped samples are quite high compared to the undoped samples of MPB composition. This is due to soft nature of the dopants which facilitates the easy reorientation of dipoles in the presence of a d.c. electric field. The d_{33} value of lanthanum doped samples decreases with increase in lanthanum concentration. The same trend is observed in case of neodymium doped samples. The combined dopants of both lanthanum and neodymium (0.01 mole each) produced the d_{33} value in between the values for lanthanum and neodymium (0.02 moles) doped samples.

TABLE 1 Ferroelectric, piezoelectric and dielectric properties of undoped PZT samples

Composition (Zr/Ti) ratio	Pr ($\mu C/cm^2$)	Ps ($\mu C/cm^2$)	Ec (V)	d_{33} (pC/N)	K
48/52	1.05	4.1	621	37	234
50/50	2.56	6.61	773	56	238
52/48	11.45	16.99	902	103	274
54/46	16.75	20.51	942	118	298

TABLE 2 Ferroelectric, piezoelectric and dielectric properties of doped PZT samples

PZT sample	Pr ($\mu C/cm^2$)	Ps ($\mu C/cm^2$)	Ec (V)	d_{33} (pC/N)	K
La(2/53/47)	18.63	24.73	1523	273	1009
La(4/53/47)	13.6	19.45	1277	224	762
La(8/53/47)	12.66	18.28	1133	208	710
Nd(2/53/47)	14.65	20.51	1313	246	664
Nd(4/53/47)	13.59	19.45	1289	197	640
La/ Nd (1/1/53/47)	15.7	21.8	1312	257	980

Dielectric constant of undoped samples was very less compared to the doped ones. This may be due to the decrease of hole conductivity by addition of soft dopants (ref.1). Dielectric constant of lanthanum doped samples decreases with increase in lanthanum concentration. This could be explained by instability of long range ferroelectric order in the material with increase in lanthanum concentration (ref.52). Generally, the stability of a spontaneously polarized ferroelectric phase requires a permanent dipole moment as well as coupling between them. The increase in lanthanum concentration may break the transnational symmetry of the polarization, favoring the establishment of local dipoles. These local dipoles are weakly coupled with each other and suppress the long-range ferroelectric order in side the material which consequently decreases the dielectric constant.

3.3. Hysteresis loop

P-E hysteresis loops of undoped and Lanthanum, neodymium doped PZTs were traced and are presented in Fig.4. From Fig. 4(A), it is observed that remnant polarization (Pr) increases with increase in zirconia concentration. The increase in zirconia concentration generally changes the tetragonal nature of the peak into a rhombohedral one. The tetragonal structure is not easily switched under the influence of an external field [29]. So, it could not lead to an expansion of the ferroelectric domain walls due to high tension state at the limit region of domain walls. But, the rhombohedral phase could cause sufficient polarization at a moderate external field with increase of the volume of domain walls and consequently increases the total polarization in the sample.

The P-E hysteresis characteristic curves of PZTs doped with lanthanum is presented in Fig.4(B). It is observed that lanthanum (0.02 moles) modified PZT at MPB composition gives maximum remanant polarization (Pr) of 18.63 $\mu C/cm^2$. This value gradually decreased with increase in dopant concentration. It is known that 'P_r" reflects the internal polarizability of ferroelectric material. Therefore, lower the P_r, lower is the polarizability. It is also known that the Curie temperature decreases with the increase in dopant concentration. Therefore, lowering of the P_r value can be attributed due to lowering of Curie temperature, which may lowers, the polarizability.

The same trend is also observed in case of neodymium doped samples (Fig.4C). Neodymium (0.02 mole) doped sample has got a maximum remnant polarization (Pr) of 14.65 $\mu C/cm^2$ which is lower than its lanthanum counterpart. The addition of both lanthanum and neodymium (0.01mole each) in the composition gives Pr value of 15.7 $\mu C/cm^2$ which is in between the values obtained in case of pure lanthanum (0.02 mole) and neodymium (0.02mole) compositions (Fig.4D).

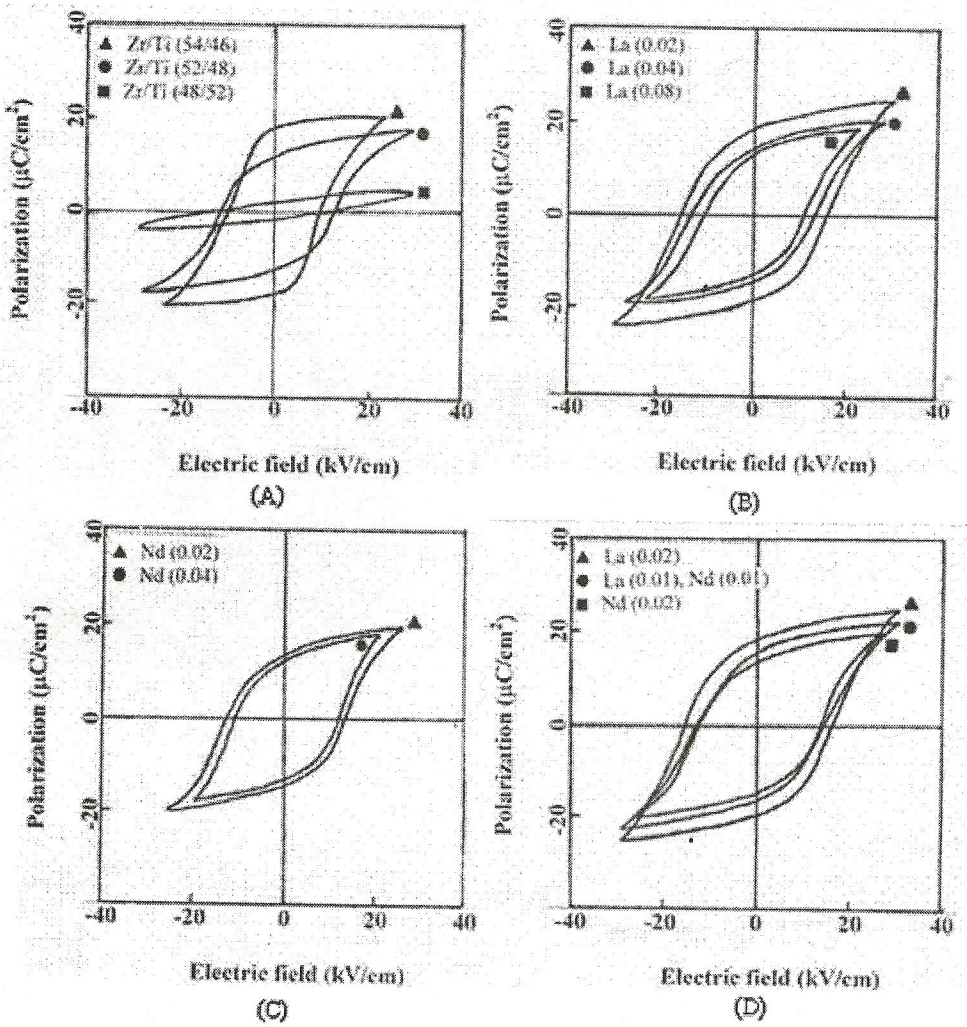

Fig.4 Hysteresis loops of (A) undoped PZT samples, (B) Lanthanum doped, (C) Neodymium doped and (D) both La, Nd doped samples.

PROPERTIES OF NAL PZT-5A AND 5H GRADE POWDERS

PZT powders of 5A and 5H grade were prepared by optimizing the Zr:Ti ratio as well as suitable dopant with suitable concentration. The properties of these powders were presented in **Table-3.**

TABLE 3.Properties of in house prepared PZT powders

PROPERTIES	NAL-5A	NAL-5H
Density (gm/cc)	7.6-7.7	7.6-7.7
Piezoelectric charge constant d_{33} (pC/N)	375-430	590-610
Relative dielectric constant (K)	1250-1330	1700-1790
Dissipation Factor (tanδ)	0.025-0.042	0.025-0.035
Particle size (median diameter, d50) µm	0.6-1.2	

5. RESULT AND DISCUSSION (PMN)

5.1. X-Ray analysis

From XRD patterns presented in Fig.5 a phase pure columbite formation is observed with 3% excess MgO. SEM micrograph of columbite powder with 3% excess MgO is shown in Fig.6, which indicates the oval shaped particles typically in the sub-micron range.

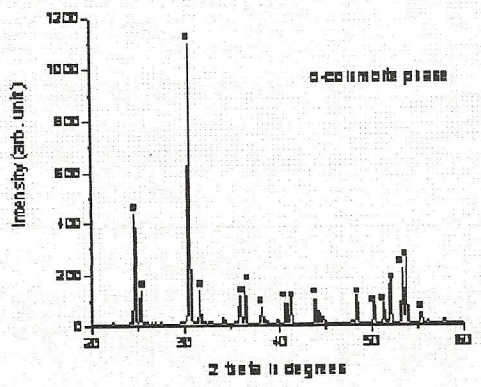

Fig.5 XRD of columbite powder

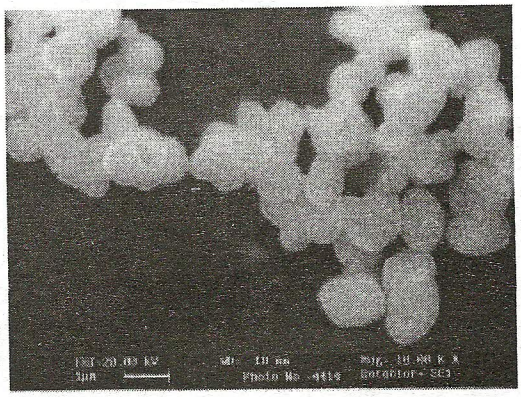

Fig.6 SEM of columbite powder

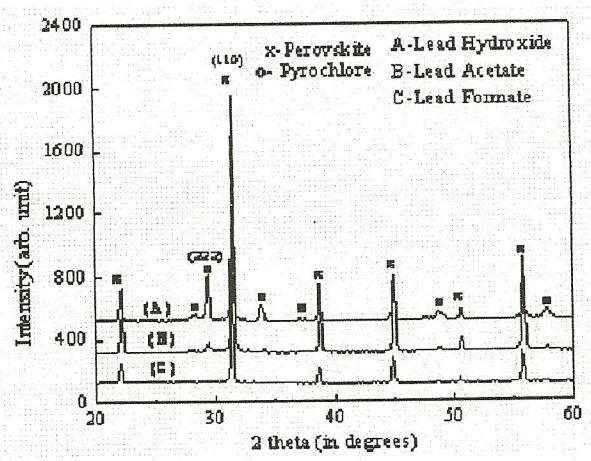

Fig.7. XRD pattern of PMN powders with different lead precursors using 3% excess MgO.

The XRD patterns of PMN powders prepared by columbite methods with 3% excess MgO are presented in Fig.7. The amount of pyrochlore phase present in each calcined powder was calculated from the intensities of the major x-ray reflections of pyrochlore phase as well as perovskite phase using the equation as proposed by Swart and Shrout [33]

$$\% \text{ of Pyrochlore} = \frac{I(\text{pyro})}{I(\text{perovskite}) + I(\text{pyro})} \times 100$$

Where, I (perovskite) refers to the intensity of the {110} plane of perovskite peak and I (pyro) refers to the intensity of the {222} plane of pyrochlore peak, these being the most intense reflections of both phases. The results are presented in Table 4. It is observed that pyrochlore free PMN powder is obtained in case of formate precursor while some residual pyrochlore phase is noticed in other two cases. The excess MgO during the columbite formation helps in the formation of pyrochlore free PMN ensuring the absence of free Nb_2O_5.

TABLE 4: % of pyrochlore in three different lead precursors

Precursors	% pyrochlore
Lead hydroxide	10.5
Lead acetate	5.6
Lead formate	0

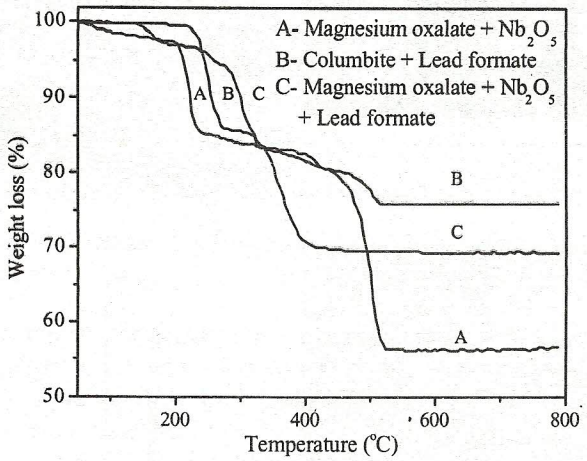

Fig.8. TGA curves of (A) Magnesium oxalate+Nb_2O_5, (B) Columbite+ Lead formate, (C) Magnesium oxalate+ Nb_2O_5+ Lead formate

Thermo gravimetric analysis (TGA)

Thermo gravimetric analysis of different compositions corresponding to (a) columbite (magnesium oxalate + Nb_2O_5) and (b) columbite + lead formate (3% excess MgO) are presented in Fig.8. In case of columbite (Fig.11A), the weight loss is due to loss of moisture (70-180°C), dehydration of magnesium oxalate (210-240°C) and the decomposition of magnesium oxalate (400-520°C) as per the equation given below.

$$MgC_2O_4 \xrightarrow{400\text{-}520^\circ C} MgO + CO + CO_2$$

Similarly, TGA study of a mixture of columbite and lead formate with 3% excess MgO shows the loss due to dehydration (225-285°C) and decomposition of lead formate (300-425°C) according to the following reaction.

$$Pb(HCOO)_2 \xrightarrow{300\text{-}425^\circ C} PbO + CO_2 + H_2O$$

Microstructure and particle size analysis

SEM picture of the calcined PMN powder prepared from lead formate precursor is shown in Fig.9. It is observed that the primary PMN particles are in sub micrometer range and due to their fineness they are agglomerated typically in the range of 1.0 to 1.3 microns. A typical particle size distribution of pyrochlore free PMN powder is shown in Fig.10. The d_{50} of the agglomerated powder is found to be around 1.2 µm. The microstructure of a sintered PMN body is shown in Fig.11. The grain size is in the range of 2-3µm. The large grain size confirms the absence of pyrochlore phase, which generally forms at grain boundary region and inhibits the grain growth of PMN particles.

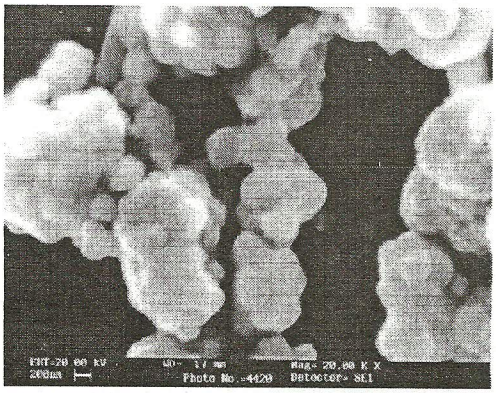

Fig.9 Typical SEM picture of PMN powder

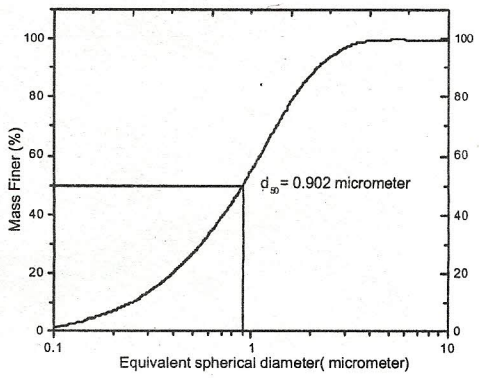

Fig.10 Typical particle size distribution curve of PMN powder

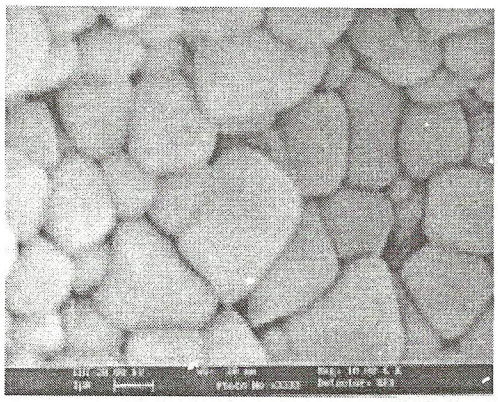

Fig.11 Typical SEM picture of PMN sintered body

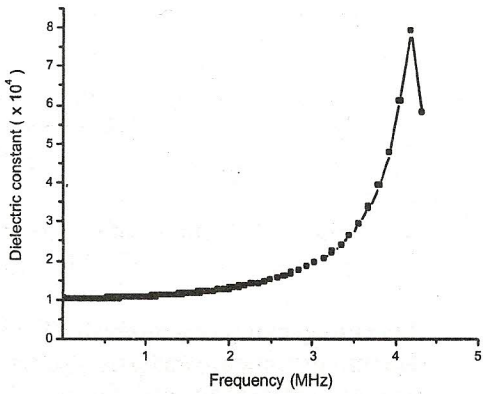

Fig.12 Dielectric constant vs. frequency graph of PMN sintered body at room temperature

Dielectric Constant

The variation in dielectric constant with change in frequency ranging from 100Hz-5MHz is shown in Fig.12. It is observed that the room temperature dielectric constant is 10,335 at 100Hz, which is in good agreement with the reported values (ref.26,51). The highest dielectric constant is 79,098 at a frequency of 4.18 MHz.

FABRICATION OF MULTILAYERED STACK

For the fabrication of multilayered stacks, the above PZT powders were uniaxially pressed in to a number of rectangular blocks of dimension 26x21x14 mm^3. The green blocks were sintered in a lead rich atmosphere to get good sintered density. The sintered blocks were cut into thin strips and were leveled, polished, electroded by using silver paste and poled in a dc field of 2kV/mm in a silicone oil bath. Strips having nearly equal d_{33} values were selected for fabrication of multi layered stack. The internal electrodes were designed in such a way so that they do not extend to the edge of the components, except for the end terminals. Layering / stacking of the strips was done carefully so that alternate layers were connected to the same terminals i.e. positive or negative without having any connections between positive and negative layers. A typical figure of a multi-layered stack of 25 layers each of 0.5mm thick is shown in Fig.13.

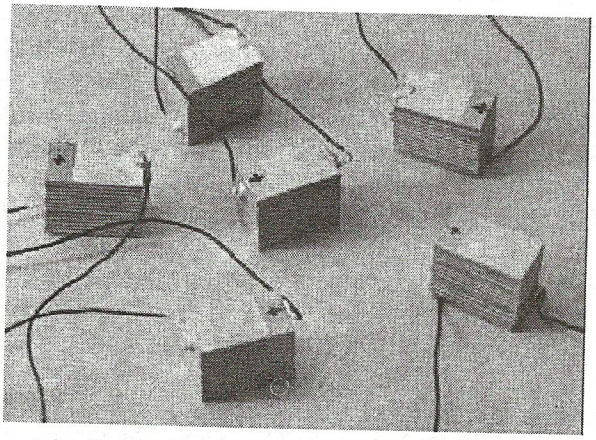

Fig.13 Typical photographs of PZT multilayered stack/ actuator.

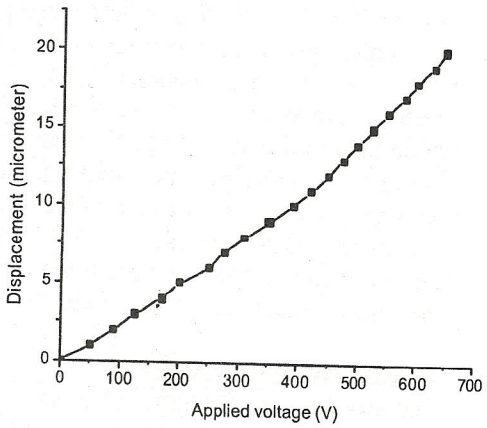

Fig.14 Displacement of a multi-layered stack as the function of applied voltage

The static displacement of fabricated multilayered stack / actuator was measured without application of mechanical load. The stack was placed on a plane rigid support on top of which the tip of the strain gauge was placed with the initial reading set at zero. The terminals of the stack were connected to appropriate terminals of a d.c source and the voltage was gradually increased. It was observed that the free strain was linear with respect to applied voltage (ref.54,55). A maximum free strain of 20μm was measured at 650V. A typical graph of free strain vs voltage is presented in Fig.14. The induced strain was found to be 0.1% of the total length of the stack/ actuator at 650V.

Critical comme nts

From the above experiment it could be seen that a high d.c. voltage of 650V is necessary to obtain a free strain of 0.1%. For a multilayered stack, the strain/ displacement can be related by the equation,

$$\delta t = n \times d_{33} \times V$$

Where, δt= displacement of the stack

n= number of layers in the stack

d_{33}= linear piezoelectric charge coefficient of the PZT material, V= applied voltage

From the above equation, it could be seen that the applied voltage is inversely proportional to the number of layers (n) of the stack, keeping 8t and d_{33} constant. So, increase in number of layers means decrease the thickness of each layer. Therefore, the applied voltage/ driving voltage will be less for thinner strips. For all practical applications, a low driving voltage (<100V) is preferable. Therefore the thickness of each layer has to be in the range of 20-50μm. This could be possible by tape casting technique.

CONCLUSIONS

PZT powders of 5A and 5H grade were successfully prepared by optimizing the Zr:Ti ratio as well as suitable dopant with appropriate concentration. From MPB compositions studies it is concluded that the rhombohedral rich phase is desirable for better piezo properties and for maximum remnant polarization .The effect of dopants on dielectric, ferroelectric and piezoelectric properties were explained on the basis of the results obtained. The piezoelectric charge coefficient (d_{33}) increases with addition of dopants. Between lanthanum and neodymium, lanthanum produces better piezoelectric and polarization properties than neodymium for the same concentration of dopants. The values gradually decrease with increase in dopant concentration. The sample having both lanthanum and neodymium (0.01 mole each) has d_{33} value is in between the values obtained in case of pure lanthanum and neodymium compositions.

Pyrochlore free PMN powders were prepared via modified columbite route.The percentage of pyrochlore phase were evaluated and compared for different lead precursors used, by referring to the most intense reflections {110} for perovskite peak and {222} for pyrochlore peak. The formate precursors in the presence of excess MgO produces pyrochlore free PMN. The large grain size in the sintered PMN is due to the absence of the grain growth inhibitor pyrochlore in the grain boundaries. The room temperature dielectric constant of PMN obtained from the lead formate precursor was found to be 10,335 at 100Hz. A maximum dielectric constant of 79,098 was measured at a frequency of 4.18MHz.

Few multilayered stacks were fabricated and their performance was evaluated. The free strain and the displacement were found to be 20 μm and 0.1% respectively at 650V.

ACKNOWLEDGEMENTS

The authors are very grateful to Dr.S.Usha Devi for XRD patterns, Mr. P.S.Laxmi Narasimham for extending the poling facilities and to Mrs.Kalavati for help in SEM studies. The authors also gratefully acknowledge Dr.T.G.Ramesh, Head, Materials Science Division and Dr.A.R.Upadhya, Director, NAL for encouraging during the course of this study. The authors also thank National Programme on Smart Materials (NPSM) for the funding.

REFERENCES

1. B. Jaffe, H. Jaffe and W.R. Cook, Piezoelectrics Ceramics. pp123-238, Academic Press, London 1971.
2. K. Kakegawa, O. Matsunaga, T. Kato and Y. Sasaki, *J. Am. Ceram. Soc*, **78,** 1071 (1995).
3. M.R. Soares, A.M.R Senos and P.Q. Mantas, *J. Eur. Ceram. Soc*, **20,** 321 (2000).
4. A.S. Bhalla, R.Guo and E.F.Alberta, *Mat.Lett*, **54,** 264 (2002).
5. P. Ari-Gur and L. Benguigui, *Sol. Stat. Commun*, **15**, 1077 (1974).
6. V.A. Isupov, *Sov. Phys. -Sol. State*, **22,** 98 (1980).
7. T. Kala, *Phys. Stat. Sol*, **78,** 277 (1983).
8. A.Barbulescu, E. Barbulescu and D. Barb, *Ferroelectrics,* **47**, 221 (1983).
9. G.H. Haertling, Piezoelectric and electrooptic ceramics, ch. 3, p. 157, Marcel Dekker, New York, 1986.
10. E.F. Crawley, J. De Luis, *AIAA Journal*, **25**, 1373 (1987).
11. Y. Sugawara, K. Onitsuka, S. Yoshikawa, Q. Xu, R.E. Newnham and K.Uchino, *J. Am. Ceram. Soc*, **75,** 996 (1992).
12. R.E. Newnham and G.R. Ruschau, *Am. Ceram. Soc.Bull*, **75**, 51 (1996).

13. J.F. Tressler, S. Alkoy, R.E. Newnham, J. Electroceramics. 2:4 (1998) 257-272.
14. R.E. Newnham, Edited by S.K. Majumdar, R.E. Tressler and E.W. Miller, The Pennsylvania Academy of Science, 1998.
15. R.E. Newnham, L.J. Bowen, K.A. Klicker and L.E. Cross, *Materials in Engineering*, **2,** 93 (1980).
16. J. Wallaschek, *J. Intell. Mat. Syst. Structures,* **6**, 71 (1995).
17. S.H. Chang and H.C. Wang., *Sensors and Actuators A*, **24**, 239 (1990).
18. B. Jaffe, R.S. Roth and S. Marzullo, *J. Appl. Phys*, **25**, 809 (1954).
19. Y. Matsuo and H. Sasaki, *J. Am. Ceram. Soc*, **48**, 289 (1965).
20. S.S. Chantreya, M. Fulath and A. Pask, *J. Am. Ceram. Soc*, **64**, 422 (1981).
21. V.R. Palkar and M.S. Multani, *Mat. Res. Bull*, **14**, 1353 (1979).
22. S. Bhattacharjee, M.K. Paria and H.S. Maiti, *Mater. Lett*, **13**, 130 (1992).
23. K. Rao, A.V. Rao and S. Komarneni, *Mater. Lett*, **28**, 463 (1996).
24. L. Guo, A. Lyashchenko and X.L. Dong, *Mater. Lett*, **56**, 849 (2002).
25. B. W. Lee, *J. Eur. Ceram. Soc*, **24**, 925 (2004).
26. B. Sahoo, V.A. Jaleel, P.K. Panda Mat. Sci. Engg.B, **126**, 80 (2006).
27. S.L Swartz., T.R. Shrout, W.A. Schulze and L.E. Cross, *J. Am. Ceram. Soc*, **67**, 311 (1984).
28. S.Nomura and K.Uchino, *Ferroelectrics*, **41**, 117 (1982).
29. K. Uchino, *Am. Ceram. Soc. Bull*, **65**, 647 (1986).
30. T.R. Shrout and A. Halliyal, *Am. Ceram. Soc. Bull*, **66**, 704 (1987).
31. J. Chen and M.P Harmer, *J. Am. Ceram. Soc*, **73**, 68 (1990).
32. M. Lejeune and J.P. Boilot, *Ceram. Int*, **8**, 99 (1982).
33. S.L. Swartz and T.R. Shrout, *Mater. Res. Bull*, **17**, 1245 (1982).
34. K. Singh and S.A. Band, *Ferroelectric*, **175**, 193 (1996).
35. S. Ananta and N.W Thomas, *J. Eur. Ceram. Soc*, **19** 155 (1999).
36. P.K. Panda and B. Sahoo, Mater. Chem.Phys, **93**, 231 (2005).
37. D.Saha, A. Sen and H.S. Maiti, *Ceram. Int*, **25**, 145 (1999).
38. A.A. Cavalheiro, S.M. Barrionuevo, J.C. Bruno, M.A. Zaghete, M. Cilense and J.A. Varela, *Mater. Chem. Phys*, **84** 107 (2004).
39. F. Chaput and J.P. Boilot, *J. Am. Ceram. Soc*, **72**, 1355 (1989).
40. L.F. Francis, Y.J. Oh and D.A. Payne, *J. Mater. Sci*, **25**, 5007 (1990).
41. K.H. Yoon, J.H. Park and D.H. Kang , *J. Am. Ceram. Soc*, **78**, 2267 (1995).
42. Y. Yoshikawa and K. Uchino, *J. Am. Ceram. Soc*, **79**, 2417 (1996).
43. Y. Narendar and G.L. Messing , *J. Am. Ceram. Soc*, **82**, 1659 (1999).
44. J.C. Carvalho, C.O.P. Santos, M.A. Zaghete, C.F. Oliveria and J.A. Varela, *J. Mater. Res*, **11**, 1795 (1996).
45. M.M.A. Sekar, A. Halliyal and K.C. Patil, *J. Mater. Res*, **11**, 1210 (1996).
46. K.H. Yoon, Y.S. Cho, D.H. Lee and D.H. Kang., *J. Am. Ceram. Soc*, **76**, 1373 (1993).
47. S.M. Gupta and A.R. Kulkarni, *J. Eur. Ceram. Soc*, **16** 473 (1996).
48. E.R. Camargo, M. Kakihana, E. Longo and E.R. Leite, *J. Alloys comp*., **314**, 140 (2001).
49. A.A. Cavalheiro, C.R. Foschini, , M.A. Zaghete, C.O. Paiva-Santos, M. Cilense, J.A. Varela and E. Longo, *Ceram. Int*, **27**, 509 (2001).
50. D. Saha, A.Sen and H.S. Maiti, *Ceram. Int*, **25**, 145 (1999).
51. D.E.Dausch and G.H.Heartling, *J. Mater. Sci*, **31**, 3409 (1996).
52. X. Dai, A. Digiovanni and D. Viehland, *J. Appl. Phys*, **74**, 3399 (1993).
53. M. Koyuncu and S.M. Pilgrim, *J. Am. Ceram. Soc*, **82**, 3075 (1999).
54. R.S. Nasar, M. Cerqueira, E. Longo, J.A. Varela and A. Beltran, *J. Eur. Ceram. Soc*, **22**, 209 (2002).
55. S. Takahasi, T. Yano, I. Fukui and E. Sato, *Jpn. J. Appl. Phys*, **24**, 206 (1985).